Faculty of Engineering, Computer and Mathematical Sciences
SCHOOL OF MECHANICAL ENGINEERING

Ocean acoustic interferometry

DOCTORAL THESIS

12th October 2008

Author: Laura A. Brooks

Supervisor:	Assoc. Prof. Anthony C. Zander †
Co-supervisors:	Dr Peter Gerstoft ††
	Prof. Colin H. Hansen †
	Dr Z. Yong Zhang *

†School of Mechanical Engineering, The University of Adelaide, Australia
††Marine Physical Laboratory, Scripps Institution of Oceanography, USA
*Defence Science and Technology Organisation, Edinburgh, Australia

References

[1] L. M. Brekhovskikh. *Waves in layered media*. Academic Press, 1960. (*Cited on pages 1, 38, and 84*)

[2] R. J. Urick. *Principles of Underwater Sound*. McGraw-Hill Book Company, 1983. (*Cited on page 1*)

[3] H. Medwin and C. S. Clay. *Fundamentals of Acoustical Oceanography*. Academic Press, San Diego, 1998. (*Cited on pages 1 and 14*)

[4] F. B. Jensen, W. A. Kuperman, M. B. Porter, and H. Schmidt. *Computational Ocean Acoustics*. Springer-Verlang New York, Inc., Fifth Avenue, New York, NY 10010, USA, 2000. (*Cited on pages 1, 15, 16, 18, 20, 21, 22, 38, 74, and 189*)

[5] P. C. Etter. *Underwater Acoustic Modeling*. E & FN SPON, 1996. (*Cited on pages 1, 19, 20, 21, and 22*)

[6] O. Diachok, A. Caiti, P. Gerstoft, and H. Schmidt, editors. *Full field inversion methods in ocean and seismo-acoustics*. Springer, 1995. (*Cited on page 1*)

[7] O. I. Lobkis and R. L. Weaver. On the emergence of the Green's function in the correlations of a diffuse field. *J. Acoust. Soc. Am.*, 110 (6):3011–3017, December 2001. (*Cited on pages 2, 28, 29, and 30*)

[8] R. L. Weaver and O. I. Lobkis. Ultrasonics without a source: Thermal fluctuation correlations at MHz frequencies. *Phys. Rev. Lett.*, 87(13): 134301–1–134301–4, September 2001. (*Cited on pages 2, 30, and 150*)

[9] A. E. Malcolm, J. A. Scales, and B. A. van Tiggelen. Extracting the Green function from diffuse, equipartitioned waves. *Phys. Rev. E.*, 70: 015601, 2004. (*Cited on pages 2 and 30*)

[10] K. van Wijk. On estimating the impulse response between receivers in a controlled ultrasonic experiment. *Geophysics*, 71(4):SI79–SI84, July–August 2006. (*Cited on pages 2 and 30*)

[11] P. Roux, K. G. Sabra, W. A. Kuperman, and A. Roux. Ambient noise cross correlation in free space: Theoretical approach. *J. Acoust. Soc. Am.*, 117(1):79–84, January 2005. (*Cited on pages 2, 44, 82, 86, and 122*)

[12] M. Campillo and A. Paul. Long-range correlations in the diffuse seismic coda. *Science*, 299:547–549, January 2003. (*Cited on pages 2, 30, 82, and 98*)

[13] R. Snieder. Extracting the Green's function from the correlation of coda waves: A derivation based on stationary phase. *Phys. Rev. E.*, 69 (4):046610–1–8, 2004 2004. (*Cited on pages 2, 25, 30, 39, 44, 86, 120, and 122*)

[14] N. M. Shapiro, M. Campillo, L. Stehly, and M. H. Ritzwoller. High-resolution surface-wave tomography from ambient seismic noise. *Science*, 307:1615–1618, March 2005. (*Cited on pages 2 and 30*)

[15] K. G. Sabra, P. Roux, and W. A. Kuperman. Arrival-time structure of the time-averaged ambient noise cross-correlation function in an oceanic waveguide. *J. Acoust. Soc. Am.*, 117(1):164–174, January 2005. (*Cited on pages 2, 3, 4, 30, 33, 35, 36, 39, 44, 48, 49, 60, 85, 86, 122, 123, and 150*)

[16] P. Gerstoft, K. G. Sabra, P. Roux, W. A. Kuperman, and M. C. Fehler. Green's functions extraction and surface-wave tomography from microseisms in southern California. *Geophysics*, 71(4):SI23–SI31, July-August 2006. (*Cited on pages 2, 25, 28, 94, and 99*)

[17] K. Wapenaar and J. Fokkema. Green's function representations for seismic interferometry. *Geophysics*, 71(4):SI33–SI46, July–August 2006. (*Cited on pages 2 and 30*)

[18] Y. Yang, M. H. Ritzwoller, A. L. Levshin, and N. M. Shapiro. Ambient noise Rayleigh wave tomography across Europe. *Geophys. J. Int.*, 168: 259–274, 2007. (*Cited on pages 2, 30, and 99*)

[19] F. Lin, M. H. Ritzwoller, J. Townend, S. Bannister, and M. K. Savage. Ambient noise Rayleigh wave tomography of New Zealand. *Geophys. J. Int.*, 170(2):649–666, August 2007. (*Cited on pages 2 and 30*)

[20] E. Larose, A. Khan, Y. Nakamura, and M. Campillo. Lunar subsurface investigated from correlation of seismic noise. *Geophys. Res. Lett.*, 32 (16):L16201, 2005. (*Cited on pages 2 and 30*)

[21] K. G. Sabra, S. Conti, P. Roux, and W. A. Kuperman. Passive *in vivo* elastography from skeletal muscle noise. *Appl. Phys. Lett.*, 90:194101, May 2007. (*Cited on pages 2 and 30*)

[22] G. M. Wenz. Acoustic ambient noise in the ocean: Spectra and sources. *J. Acoust. Soc. Am.*, 34(12):1936–1956, December 1962. (*Cited on pages 2 and 83*)

[23] R. J. Urick. *Principles of Underwater Sound*. McGraw-Hill, New York, 1975. (*Cited on pages 2 and 83*)

[24] M. R. Loewen and W. K. Melville. A model of the sound generated by breaking waves. *J. Acoust. Soc. Am.*, 90(4):2075–2080, October 1991. (*Cited on pages 2 and 83*)

[25] P. Roux, W. A. Kuperman, and the NPAL Group. Extracting coherent wave fronts from acoustic ambient noise in the ocean. *J. Acoust. Soc. Am.*, 116(4):1995–2003, October 2004. (*Cited on pages 3, 4, 34, 82, 86, and 150*)

[26] L. A. Brooks and P. Gerstoft. Ocean acoustic interferometry of 20–100 Hz noise. *J. Acoust. Soc. Am.*, Submitted 2008. (*Cited on pages 3, 36, and 81*)

[27] K. G. Sabra, P. Roux, A. M. Thode, G. D'Spain, W. S. Hodgkiss, and W. A. Kuperman. Using ocean ambient noise for array self-localization and self-synchronization. *IEEE J. Ocean. Eng.*, 30(2):338–347, April 2005. (*Cited on pages 3, 5, 7, 33, 99, and 157*)

[28] A. Curtis, P. Gerstoft, H. Sato, R. Snieder, and K. Wapenaar. Seismic interferometry–turning noise into signal. *The Leading Edge*, 25:1082–1092, September 2006. (*Cited on pages 3, 30, and 35*)

[29] P. Roux and M. Fink. Green's function estimation using secondary sources in a shallow water environment. *J. Acoust. Soc. Am.*, 113(3): 1406–1416, March 2003. (*Cited on pages 4, 32, 35, 37, 59, and 63*)

[30] R. Snieder, K. Wapenaar, and K. Larner. Spurious multiples in seismic interferometry of primaries. *Geophysics*, 71(4):SI111–SI124, July-August 2006. (*Cited on pages 4, 35, 36, 37, 39, 44, 48, 49, 51, 60, 84, 85, and 120*)

[31] C. C. Leroy and F. Parthiot. Depth-pressure relationships in the oceans and seas. *J. Acoust. Soc. Am.*, 103(3):1346–1352, March 1998. (*Cited on page 10*)

[32] H. Medwin. Speed of sound in water: A simple equation for realistic parameters. *J. Acoust. Soc. Am.*, 58(6):1318–1319, December 1975. (*Cited on page 10*)

[33] V. A. Del Grosso. New equation for the speed of sound in natural waters (with comparisons to other equations). *J. Acoust. Soc. Am.*, 56 (4):1084–1091, October 1974. (*Cited on page 10*)

[34] K. V. Mackenzie. Nine-term equation for sound speed in the oceans. *J. Acoust. Soc. Am.*, 70:807–812, 1981. (*Cited on page 10*)

[35] F. H. Fisher and V. P. Simmons. Sound absorption in sea water. *J. Acoust. Soc. Am.*, 62(3):558–564, September 1977. (*Cited on page 12*)

[36] R. E. Francois and G. R. Garrison. Sound absorption based on ocean measurements. Part II: Boric acid contribution and equation for total absorption. *J. Acoust. Soc. Am.*, 72(6):1879–1890, December 1982. (*Cited on pages 12 and 13*)

[37] M. A. Ainslie and J. G. McColm. A simplified formula for viscous and chemical absorption in sea water. *J. Acoust. Soc. Am.*, 103(3): 1671–1672, March 1998. (*Cited on page 12*)

[38] F. B. Jensen. Wave theory modeling: A convenient approach to CW and pulse propagation modeling in low-frequency acoustics. *IEEE J. Ocean. Eng.*, 13(4):186–196, October 1988. (*Cited on page 14*)

[39] J. A. Ogilvy. Wave scattering from rough surfaces. *Rep. Prog. Phys.*, 50:1553–1608, 1987. (*Cited on page 14*)

[40] MIT OpenCourseWare site. URL `http://ocw.mit.edu`. (*Cited on page 16*)

[41] P. M. Morse and K. U. Ingard. *Theoretical acoustics*. Princeton University Press, 1986. (*Cited on page 18*)

[42] M. B. Porter and H. P. Bucker. Gaussian beam tracing for computing ocean acoustic fields. *J. Acoust. Soc. Am.*, 82(4):1349–1359, October 1987. (*Cited on page 19*)

[43] H. P. Bucker. A simple 3-D Gaussian beam sound propagation model for shallow water. *J. Acoust. Soc. Am.*, 95(5):2437–2440, May 1994. (*Cited on page 19*)

[44] J. S. Perkins and R. N. Baer. An approximation of the three-dimensional parabolic equation method for acoustic propagation. *J. Acoust. Soc. Am.*, 72(2):515–522, August 1982. (*Cited on page 22*)

[45] H. P. Bucker. An equivalent bottom for use with the split-step algorithm. *J. Acoust. Soc. Am.*, 73(2):486–491, February 1983. (*Cited on page 22*)

[46] D. Lee and S. T. McDaniel. A finite-difference treatment of interface conditions for the parabolic wave equation: The irregular interface. *J. Acoust. Soc. Am.*, 73(5):1441–1447, May 1983. (*Cited on page 22*)

[47] R. A. Stephen. Solutions to range-dependent benchmark problems by the finite-difference method. *J. Acoust. Soc. Am.*, 87(4):1527–1534, April 1990. (*Cited on page 23*)

[48] M. Porter. *The KRAKEN normal mode program*. Saclantcen Memorandum: SM-245, September 1991. (*Cited on pages 23 and 74*)

[49] H. Schmidt. *OASES Version 3.1 User Guide and Reference Manual*. Department of Ocean Engineering, Massachusetts Institute of Technology, October 2004. (*Cited on pages 23, 52, 72, 96, 126, and 154*)

[50] J. F. Claerbout. Synthesis of a layered medium from its acoustic transmission response. *Geophysics*, 33(2):264–269, April 1968. (*Cited on page 24*)

[51] J. F. Claerbout. *Fundamentals of geophysical data processing*. Blackwell, 1976. (*Cited on page 24*)

[52] J. Rickett and J. Claerbout. Acoustic daylight imaging via spectral factorization: helioseismology and reservoir monitoring. *The Leading Edge*, 18(8):957–960, 1999. (*Cited on page 24*)

[53] T. L. Duvall Jr, S. M. Jefferies, J. W. Harvey, and M. A. Pomerantz. Time-distance helioseismology. *Nature*, 362:430–432, April 1993. (*Cited on page 24*)

[54] C. R. Farrar and G. H. James III. System identification from ambient vibration measurements on a bridge. *J. Sound Vib.*, 205(1):1–18, August 1997. (*Cited on page 24*)

[55] P. Roux, K. G. Sabra, P. Gerstoft, W. A. Kuperman, and M. C. Fehler. P-waves from cross correlation of seismic noise. *Geophys. Res.Lett.*, 32: L19303, 2005. (*Cited on page 25*)

[56] A. Derode, E. Larose, M. Tanter, J. de Rosny, A. Tourin, M. Campillo, and M. Fink. Recovering the Green's function from field-field correlations in an open scattering medium. *J. Acoust. Soc. Am.*, 113(6): 2973–2976, June 2003. (*Cited on pages 30, 37, 86, and 150*)

[57] K. Wapenaar. Retrieving the elastodynamic Green's function of an arbitrary inhomogeneous medium by cross correlation. *Phys. Rev. Lett.*, 93(25):254301–1–254301–4, December 2004. (*Cited on page 30*)

[58] D.-J. van Manen, J. O. A. Robertsson, and A. Curtis. Modeling of wave propagation in inhomogeneous media. *Phys. Rev. Lett.*, 94(16): 164301–1–164301–4, April 2005. (*Cited on page 30*)

[59] E. Larose, A. Derode, M. Campillo, and M. Fink. Imaging from one-bit correlations of wideband diffuse wavefields. *J. Appl. Phys.*, 95: 8393–8399, 2004. (*Cited on pages 30 and 99*)

[60] P. Gerstoft, K. Sabra, P. Roux, W. A. Kuperman, and W. S. Hodgkiss. Passive acoustic and seismic tomography with ocean ambient noise in ORION. In *Proceedings of the International Conference "Underwater Acoustic Measurements: Technologies & Results" Heraklion, Crete, Greece*, 28 June – 1 July 2005. (*Cited on page 30*)

[61] K. G. Sabra, P. Gerstoft, P. Roux, and W. A. Kuperman. Extracting time-domain Green's function estimates from ambient seismic noise. *Geophys. Res. Lett.*, 32:L03310, 2005. (*Cited on pages 30 and 102*)

[62] G. D. Bensen, M. H. Ritzwoller, M. P. Barmin, A. L. Levshin, F. Lin, M. P. Moschetti, N. M. Shapiro, and Y. Yang. Processing seismic ambient noise data to obtain reliable broad-band surface wave dispersion measurements. *Geophys. J. Int.*, 169:1239–1260, 2007. (*Cited on pages 30, 96, 99, and 102*)

[63] K. G. Sabra, E. S. Winkel, D. A. Bourgoyne, B. R. Elbing, S. L. Ceccio, M. Perlin, and D. R. Dowling. Using cross correlations of turbulent

flow induced vibrations for structural health monitoring. *J. Acoust. Soc. Am.*, 121(4):1987–1995, April 2007. (*Cited on page 30*)

[64] W. A. Kuperman. Utilizing acoustic noise. In *Pacific Rim underwater acoustics conference*, 2007. (*Cited on page 31*)

[65] M. Siderius, C. H. Harrison, and M. B. Porter. A passive fathometer technique for imaging seabed layering using ambient noise. *J. Acoust. Soc. Am.*, 120(3):1315–1323, September 2006. (*Cited on pages 34 and 86*)

[66] P. Gerstoft, W. S. Hodgkiss, M. Siderius, C.-F. Huang, and C. H. Harrison. Passive fathometer processing. *J. Acoust. Soc. Am.*, 123(3): 1297–1305, March 2008. (*Cited on pages 34 and 86*)

[67] C. H. Harrison and M. Siderius. Bottom profiling by correlating beam-steered noise sequences. *J. Acoust. Soc. Am.*, 123(3):1282–1296, March 2008. (*Cited on page 34*)

[68] C. M. Bender and S. A. Orszag. *Advanced Mathematical Methods for Scientists and Engineers: Asymptotic Methods and Perturbation Theory*. McGraw-Hill, 1978. (*Cited on pages 38, 39, 85, and 120*)

[69] L. A. Brooks and P. Gerstoft. Ocean acoustic interferometry. *J. Acoust. Soc. Am.*, 121(6):3377–3385, June 2007. (*Cited on pages 44, 84, 85, and 86*)

[70] D. Tang, J. N. Moum, J. F. Lynch, P. Abbot, R. Chapman, P. H. Dahl, T. F. Duda, G. Gawarkiewicz, S. Glenn, J. A. Goff, H. Graber, J. Kamp, A. Maffei, J. D. Nash, and A. Newhall. Shallow water '06: A joint acoustic propagation/ nonlinear internal wave physics experiment. *Oceanography*, 20(4):156–167, December 2007. (*Cited on pages 65 and 66*)

[71] Y.-M. Jiang and N. R. Chapman. Bayesian geoacoustic inversion in a dynamic shallow water environment. *J. Acoust. Soc. Am.*, 123(6): EL155–EL161, June 2008. (*Cited on pages 65, 77, and 78*)

[72] C.-F. Huang, P. Gerstoft, and W. S. Hodgkiss. Effect of ocean sound speed uncertainty on matched-field geoacoustic inversion. *J. Acoust. Soc. Am.*, 123(6):EL162–EL168, June 2008. (*Cited on pages 65, 77, and 78*)

[73] J. A. Goff, B. J. Kraft, L. A. Mayer, S. G. Schock, C. K. Sommerfield, H. C. Olson, S. P. S. Gulick, and S. Nordfjord. Seabed characterization on the New Jersey middle and outer shelf: Correlatability and spatial variability of seafloor sediment properties. *Mar. Geol.*, 209:147–172, 2004. (*Cited on pages 67, 79, 104, and 126*)

[74] N. R. Chapman. Empirical geoacoustic model for SW06 experimental sites. Pre-cruise document, 2006. (*Cited on page 67*)

[75] A. E. Newhall, T. F. Duda, K. von der Heydt, J. D. Irish, J. N. Kemp, S. A. Lerner, S. P. Liberatore, Y.-T. Lin, J. F. Lynch, A. R. Maffei, A. K. Morozov, A. Shmelev, C. J. Sellers, and W. E. Witzell. Acoustic and oceanographic observations and configuration information for the WHOI moorings from the SW06 experiment. Technical report, Woods Hole Oceanographic Institute, May 2007. (*Cited on pages 66, 68, 191, and 198*)

[76] *SBE 9plus CTD User's manual*. Sea-Bird Electronics, Inc. URL `http://www.seabird.com`. (*Cited on page 69*)

[77] M. Badiey, Y. Mu, J. Lynch, J. Apel, and S. Wolf. Temporal and azimuthal dependence of sound propagation in shallow water with internal waves. *J. Acoust. Soc. Am.*, 27(1):117–129, January 2002. (*Cited on page 72*)

[78] C. W. Holland. Seabed reflection measurement uncertainty. *J. Acoust. Soc. Am.*, 114(4):1861–1873, October 2003. (*Cited on page 73*)

[79] A. Turgut. SW06 bottom characterization by using chirp sonar and GeoProbe data. In *Shallow Water 2006 Experiment San Diego Workshop*, 2007. (*Cited on page 78*)

[80] K. Wapenaar. Green's function retrieval by cross-correlation in case of one-sided illumination. *Geophys. Res. Lett.*, 33:L19304, October 2006. (*Cited on page 82*)

[81] K. G. Sabra, P. Gerstoft, P. Roux, W. A. Kuperman, and M. C. Fehler. Surface wave tomography from microseisms in Southern California. *Geophys. Res. Lett.*, 32:L14311, 2005. (*Cited on pages 94 and 99*)

[82] A. Derode, A. Tourin, and M. Fink. Ultrasonic pulse compression with one-bit time reversal through multiple scattering. *J. Appl. Phys.*, 85: 6343, 1999. (*Cited on page 99*)

[83] N. M. Shapiro and M. Campillo. Emergence of broadband Rayleigh waves from correlations of the ambient seismic noise. *Geophys. Res. Lett.*, 31:L07614, 2004. (*Cited on page 99*)

[84] F. J. Sánchez-Sesma and M. Campillo. Retrieval of the Green's function from cross correlation: The canonical elastic problem. *Bull. Seism. Soc. Am.*, 96(3):1182–1191, June 2006. (*Cited on page 104*)

[85] L. A. Brooks and P. Gerstoft. Experimental ocean acoustic interferometry. *J. Acoust. Soc. Am.*, Submitted 2008. (*Cited on page 118*)

[86] L. A. Brooks, P. Gerstoft, and D. P. Knobles. Multichannel array diagnosis using noise cross-correlation. *J. Acoust. Soc. Am.*, 124(4): EL203–EL209, October 2008. (*Cited on page 145*)

[87] M. Celis, J. E. Dennis, and R. A. Tapia. A trust region strategy for nonlinear equality constrained optimization. *Numerical Optimization 1994*, pages 71–82, 1985. (*Cited on pages 147 and 160*)

[88] T. F. Coleman and Y. Li. On the convergence of reflective Newton methods for large-scale nonlinear minimization subject to bounds. *Mathematical Programming*, 67(2):189–224, 1994. (*Cited on pages 147 and 160*)

[89] P. S. Wilson, J. L. Ellzey, and T. G. Muir. Experimental investigation of the combustive sound source. *IEEE J. Ocean. Eng.*, 20(4):311–320, October 1995. (*Cited on page 147*)

[90] W. S. Hodgkiss. Shape determination of a shallow-water bottomed array. In *Proc. OCEANS'89*, pages 1199–1204, 1989. (*Cited on page 157*)

[91] W. S. Hodgkiss, P. Gerstoft, and J. J. Murray. Array shape estimation from sources of opportunity. In *OCEANS 2003 Proc.*, 2003. (*Cited on page 157*)

[92] S. Dosso, N. E. B. Collison, G. J. Heard, and R. I. Verrall. Experimental validation of regularized array element localization. *J. Acoust. Soc. Am.*, 115(5):2129–2137, May 2004. (*Cited on page 157*)

[93] T. McGee, J. R. Woolsey, L. Lapham, R. Kleinberg, L. Macelloni, B. Battista, C. Knapp, S. Caruso, V. Goebel, R. Chapman, and P. Gerstoft. Structure of a carbonate/hydrate mound in the Northern Gulf of Mexico. In *6th International Conference on Gas Hydrates, Vancouver, British Columbia, Canada*, 2008. (*Cited on page 174*)

[94] T. M. McGee. Presented to the international association of oil and gas producers. Technical report, 2007. (*Cited on page 175*)

[95] W. S. Hodgkiss. DURIP: Autonomous broadband receive arrays. Technical report, Marine Physical Laboratory, Scripps Institution of Oceanography, 1997. Final Report, Contract N00014–05–1–0447. (*Cited on page 193*)

[96] SWAMI mooring diagrams supplied by ARL-UT engineers. (*Cited on pages 195 and 196*)

Appendix A

Normalisation for Impedance Changes

In order to satisfy the equal amplitude criterion of Section 3.1.2, the cross-correlations from sources that span an area of varying impedance should be normalised by dividing by $\frac{\rho_s c}{\sin\theta_s}$, as calculated at the source location, where ρ is medium density, c is medium sound speed, and θ is the grazing angle with the horizontal. This can be understood by considering the following.

Consider the geometry of Figure 3.3(a). Let R be a reflection from the bottom of the water column, R' be a reflection from the top of the sediment, R'' a reflection from the bottom of the sediment, T a transmission from the water column into the sediment, and T' a transmission from the sediment to the water column. If the source amplitude is S_a, the cross-correlation of the acoustic path from S to A with the path from S to B yields an amplitude of $S_aTT' \times S_aR$. Similarly, for the geometry of Figure 3.3(b) the cross-correlation of the paths from S' to each receiver yield an amplitude of $S_bR'T' \times S_bT'$. The two will cancel only if

$$S_aTT' \times S_aR = -S_bR'T' \times S_bT'. \tag{A.1}$$

The reflection coefficient at the interface of two media is defined as [4]

$$R_{12} = \frac{\frac{\rho_2 c_2}{\sin\theta_2} - \frac{\rho_1 c_1}{\sin\theta_1}}{\frac{\rho_2 c_2}{\sin\theta_2} + \frac{\rho_1 c_1}{\sin\theta_1}}, \tag{A.2}$$

where medium 1 is the medium in which the wave is travelling, and medium 2 is the medium on the other side of the interface. The transmission coefficient from medium 1 to 2 is

$$T_{12} = \frac{2\frac{\rho_2 c_2}{\sin\theta_2}}{\frac{\rho_2 c_2}{\sin\theta_2} + \frac{\rho_1 c_1}{\sin\theta_1}}. \tag{A.3}$$

Substituting Eq. (A.2) and Eq. (A.3) into Eq. (A.1) and simplifying yields

$$\frac{S_a^2}{\frac{\rho_a c_a}{\sin\theta_a}} = \frac{S_b^2}{\frac{\rho_b c_b}{\sin\theta_b}}, \tag{A.4}$$

where subscript a denotes the water column and subscript b denotes the sediment.

Appendix B

Array Details

Four arrays were used to collect data: MPL-VLA1, SWAMI32, SWAMI52, and Shark. The MPL-VLA1 is a vertical line array that is able to maintain its vertical configuration after deployment due to an anchor at the array bottom, and a buoyancy float at the top. The other three arrays are L-shaped, with a vertical line array (VLA) component and a horizontal line array (HLA) component. The vertical components maintain their shape due to buoyancy floats at the top and electronics modules that are heavy enough to anchor them at the bottom. The horizontal arrays are all anchored at both ends so that they retain their straight horizontal configuration. Descriptions of the SW06 array dimensions with mooring diagrams, as well as details of the data acquisition system for each array, are included in this appendix. Photographs of the arrays are included in the thesis body as Figure 4.2. All of the information in this appendix has been provided courtesy of the Marine Physical Laboratory, Scripps Institution of Oceanography (MPL-VLA1 array), Applied Research Laboratories, University of Texas at Austin (SWAMI arrays), and Woods Hole Oceanographic Institute [75] (Shark array).

B.1 Array geometries

The array geometries and mooring diagrams are detailed here. The mooring diagrams are the *a priori* experimental designs, and as such, the depth specified on each mooring diagram is different from the surveyed water depth at the experimental site.

B.1.1 MPL-VLA1 array

The MPL-VLA1 array is a 16 element VLA with elements denoted H-1–H-16. A mooring diagram of the configuration is shown in Figure B.1. During the SW06 experiments it was deployed at a depth of 79 m, at a surveyed location of 39° 01.477′ N, 73° 02.256′ W. The elements were evenly spaced vertically at 3.75 m intervals, the lowest, H-1, being 8.2 m above the seafloor.

NOTE: This figure is included on page 193 in the print copy of the thesis held in the University of Adelaide Library.

Figure B.1: MPL-VLA1 mooring diagram (source: Hodgkiss [95]).

B.1.2 SWAMI arrays

The SWAMI32 array consists of a 12 element VLA, with elements denoted H-1–H-12, and a 20 element HLA, with elements denoted H-13–H-32. A mooring diagram of the configuration is shown in Figure B.2. During the SW06 experiments it was deployed at a depth of 68.5 m, with the base of the VLA at a surveyed location of 39° 03.6180′ N, 73° 07.8970′ W. The two lowest VLA elements, H-11 and H-12, were tied off approximately 2 m above the seafloor. The other 10 VLA elements were evenly spaced at 5.95 m intervals, the lowest, H-10, being 4.65 m above the seafloor. The first HLA element, H-13, was located 7.795 m from the base of the VLA at a bearing of 224° True. The vector of distances of H-14–H-32 from H-13 in metres was [20.32, 39.66, 58.06, 75.57, 92.24, 108.10, 123.20, 137.57, 151.24, 164.25, 176.63, 188.42, 199.64, 210.31, 220.47, 230.14, 239.34, 248.10, 256.43].

The SWAMI52 array consists of a 16 element VLA, with elements denoted H-1–H-16, and a 36 element HLA, with elements denoted H-17–H-52. A mooring diagram of the configuration is shown in Figure B.3. During the SW06 experiments it was deployed at a depth of 73.8 m, with the base of the VLA at a surveyed location of 39° 12.0010′ N, 72° 57.9740′ W. The two lowest VLA elements, H-15 and H-16, were tied off approximately 2 m above the seafloor. The other 14 VLA elements were evenly spaced at 4.37 m intervals, the lowest, H-14, being 4.3 m above the seafloor. The first HLA element, H-17, was located 7.795 m from the base of the VLA at a bearing of 314° True (i.e. perpendicular to the SWAMI32 array). The vector of distances of H-18–H-52 from H-17 in metres was [15.84, 29.48, 41.21, 51.32, 60.00, 67.49, 73.94, 79.48, 84.60, 89.33, 93.70, 97.74, 101.47, 104.91, 108.09, 111.03, 113.75, 116.25, 118.97, 121.91, 125.09, 128.53, 132.26, 136.30, 140.67, 145.40, 150.52, 156.07, 162.51, 169.99, 178.69, 188.79, 200.52, 214.16, 230.00].

NOTE: This figure is included on page 195 in the print copy of the thesis held in the University of Adelaide Library.

Figure B.3: SWAMI52 mooring diagram (source: ARL-UT [96]).

NOTE: This figure is included on page 196 in the print copy of the thesis held in the University of Adelaide Library.

Figure B.3: SWAMI52 mooring diagram (source: ARL-UT [96]).

B.1.3 Shark array

The Shark L-array consists of a 16 element VLA, with elements denoted H-0–H-15, and a 32 element HLA, with elements denoted H-16–H-47. A mooring diagram of the configuration is shown in Figure B.4. During the SW06 experiments the array was deployed at a depth of 79 m, with the base of the VLA at a surveyed location of 39° 01.2627′ N, 73° 02.9887′ W. The three lowest VLA elements, H-13–H-15, were tied off 1.25 m above the seafloor. The vector of depths in metres below the sea surface of the other 12 VLA elements, H-0–H-12, was [13.5, 17.25, 21.0, 24.75, 28.5, 32.35, 36.0, 39.75, 43.5, 47.25, 54.75, 62.25, 69.75]. The HLA bearing was 1.45° True. The HLA elements, H-47–H-16, were evenly spaced at 15 m intervals, with the closest, H-47, located 3 m from the base of the VLA.

NOTE: This figure is included on page 198 in the print copy of the thesis held in the University of Adelaide Library.

Figure B.4: Shark mooring diagram (source: Newhall *et al*. [75]).

B.2 Array data acquisition specifications

Details of the data acquisition system for each array are presented in Table B.1.

	SWAMI arrays	MPL-VLA1 array	Shark array
Resolution	16 bits	16 bits	16 bits
Sampling rate	2400 Hz (SWAMI52) 6250 Hz (SWAMI32)	50 kHz	9765.625 Hz
Recording media	DAT DDS-3 (digital audio tape digital data storage)	IDE (integrated drive electronics) hard disk drive	PC/104-plus stack (PC compatible circuit board with a peripheral component interface bus addition)
Capacity	264 Gb	470 Gb	~ 4 TB
Continuous recording	8 days	116 hours	43 days
Hydrophone sensitivity	-222 dB re 1 V/µPa or -168 dB re 1 V/µPa (variable)	-198 dB re 1 V/µPa	-170 dB re 1 V/µPa
Input gain	variable: 10 dB, 30 dB, 50 dB or 70 dB	variable: 20 dB, 40 dB or 60 dB	21 dB
Frequency range	rated down to 20 Hz	20 Hz – 30 kHz	10 Hz – 10 kHz

Table B.1: Data acquisition capabilities of the SWAMI arrays, MPL-VLA1 array, and Shark array.

Appendix C

The Inversion Process

The inversion process attempts to determine a model, $\mathbf{m}$, which optimises an objective function, ϕ, for a set of physical data measurements, $\mathbf{p}$. The solution of an inverse problem has two components, namely the forward model, and the inverse model. The forward model determines the mathematical relationship between the unknown parameters to be estimated and the acoustic field. Using the measured acoustic field and the forward mathematical relationship, the inverse model determines the rule used to calculate the unknown parameters.

The inverse problem requires P data measurements, forming vector

$$\mathbf{p} = [p_1, p_2, ..., p_P]^T . \tag{C.1}$$

The Q unknown parameters to be determined form vector

$$\mathbf{q} = [q_1, q_2, ..., q_Q]^T , \tag{C.2}$$

where $P > Q$. Using the forward model, $\mathbf{p}$ is predicted for different combinations of $\mathbf{q}$. The inverse model is employed to identify values of $\mathbf{q}$ that give the best prediction of $\mathbf{p}$. As the number of measurements exceeds the number of unknown parameters, an exact solution that satisfies all N measured parameters does not generally exist. Hence, a solution that best satisfies the measured parameters must be obtained. This is done by repeatedly running the forward and inverse models with different $\mathbf{q}$ vectors, as depicted in Figure C.1, until the difference between the measured acoustic field and the field predicted by the forward model is minimised.

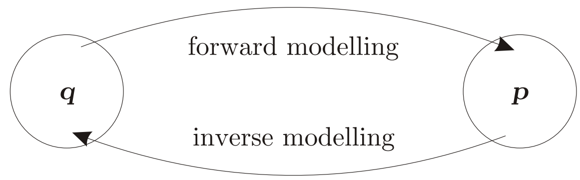

Figure C.1: The inversion process.

The inversion process can be carried out using either non-linear techniques based on full-field global optimisation, or using linear inversion techniques that match only selected features of the acoustic field with corresponding replica features, that is, features that are estimated from the inversion. These optimisation techniques seek to minimise the objective function $\phi = f(\mathbf{p}, \mathbf{q}(\mathbf{m}))$, where $\mathbf{m}$ is the set of physical parameters to be estimated.

Appendix D

Publications

Journal publications and conference proceedings that have directly resulted from the work presented in this thesis are listed here:

D.1 Journal papers

L. A. Brooks and P. Gerstoft, "Ocean acoustic interferometry," *J. Acoust. Soc. Am.* 121(6), pp. 3377–3385, June 2007.

L. A. Brooks, P. Gerstoft, and D. P. Knobles, "Multichannel array diagnosis using noise cross-correlation," *J. Acoust. Soc. Am.* 124(4), pp. EL203–EL209, October 2008.

L. A. Brooks and P. Gerstoft, "Ocean acoustic interferometry of 20–100 Hz noise," *J. Acoust. Soc. Am.* Submitted 2008.

L. A. Brooks and P. Gerstoft, "Experimental ocean acoustic interferometry," *J. Acoust. Soc. Am.* Submitted 2008.

D.2 Refereed conference papers

L. A. Brooks and P. Gerstoft, "Ocean acoustic interferometry experiment," proceedings of ICSV14, Cairns, Australia, July 2007.

D.3 Invited talks

P. Gerstoft, L. A. Brooks*, S. Fried, W. A. Kuperman, and K. G. Sabra, "Ocean acoustic interferometry using noise and active sources," AGU Fall Meeting, San Francisco, December 10–14 2007.

D.4 Other conference proceedings

L. A. Brooks and P. Gerstoft, "Green's function retrieval through ocean acoustic interferometry (A)," 153rd Meeting of the Acoustical Society of America *J. Acoust. Soc. Am.* 121(5), p. 3102, May 2007.

L. A. Brooks and P. Gerstoft, "Extracting Green's functions from noise correlation of SW06 data," Acoustics '08, Paris, June 29 – July 4, 2008.

NOTE: This figure is included in the print copy of the thesis held in the University of Adelaide Library.

source: "Piled Higher and Deeper" by Jorge Cham - www.phdcomics.com.